Journal of Hazardous Materials 190 (2011) 366–374

Contents lists available at ScienceDirect

Journal of Hazardous Materials

journal homepage: www.elsevier.com/locate/jhazmat

Paraquat-loaded alginate/chitosan nanoparticles: Preparation, characterization and soil sorption studies

Mariana dos Santos Silva[a], Daniela Sgarbi Cocenza[a], Renato Grillo[a,b], Nathalie Ferreira Silva de Melo[a,b], Paulo Sérgio Tonello[a], Luciana Camargo de Oliveira[c], Douglas Lopes Cassimiro[d], André Henrique Rosa[a], Leonardo Fernandes Fraceto[a,b,*]

[a] Department of Environmental Engineering, São Paulo State University – UNESP, Avenida Três de Março, No. 511, CEP 18087-180, Sorocaba, SP, Brazil
[b] Department of Biochemistry, Institute of Biology, State University of Campinas – UNICAMP, Campinas, SP, Brazil
[c] Department of Chemistry, UFSCAr, Campus Sorocaba, SP, Brazil
[d] Institute of Chemistry, São Paulo State University – UNESP, Araraquara, SP, Brazil

ARTICLE INFO

Article history:
Received 9 August 2010
Received in revised form 11 March 2011
Accepted 15 March 2011
Available online 23 March 2011

Keywords:
Paraquat
Nanoparticles
Alginate
Chitosan

ABSTRACT

Agrochemicals are amongst the contaminants most widely encountered in surface and subterranean hydrological systems. They comprise a variety of molecules, with properties that confer differing degrees of persistence and mobility in the environment, as well as different toxic, carcinogenic, mutagenic and teratogenic potentials, which can affect non-target organisms including man. In this work, alginate/chitosan nanoparticles were prepared as a carrier system for the herbicide paraquat. The preparation and physicochemical characterization of the nanoparticles was followed by evaluation of zeta potential, pH, size and polydispersion. The techniques employed included transmission electron microscopy, differential scanning calorimetry and Fourier transform infrared spectroscopy. The formulation presented a size distribution of 635 ± 12 nm, polydispersion of 0.518, zeta potential of -22.8 ± 2.3 mV and association efficiency of 74.2%. There were significant differences between the release profiles of free paraquat and the herbicide associated with the alginate/chitosan nanoparticles. Tests showed that soil sorption of paraquat, either free or associated with the nanoparticles, was dependent on the quantity of organic matter present. The results presented in this work show that association of paraquat with alginate/chitosan nanoparticles alters the release profile of the herbicide, as well as its interaction with the soil, indicating that this system could be an effective means of reducing negative impacts caused by paraquat.

1. Introduction

Agrochemicals have become the product class most widely encountered in surface and subterranean hydrological systems worldwide, due to their extensive use in agriculture and in urban areas. They comprise a variety of molecules possessing different properties that confer varying degrees of environmental persistence and mobility, as well as different toxic, carcinogenic, mutagenic and teratogenic potentials. They can affect the endocrine systems of non-target organisms, including humans [1]. Paraquat (1-1′-dimethyl-4-4′-bipiridyl), a non-selective contact herbicide, is a bi-quaternary ammonium compound, which is normally synthesized as the dichloride salt. It was introduced in the 1960s, and is today used in over 100 countries in plantations of tobacco, cotton, rice, coffee, sugar cane, beans, apples, soy, grapes and other crops [2]. Paraquat (as well as diquat) is also extensively used in direct sowing management systems, either alone or in mixtures with other herbicides, as well as for weed control in uncultivated areas, pasture renewal and pre-harvest drying [3]. According to the United States Environmental Protection Agency [4], the acceptable concentration limit for paraquat in drinking water is 0.03 mg L^{-1}, and the toxicity limit with respect to aquatic organisms is 15 mg L^{-1}. Its Environmental Danger Potential classification is II (very dangerous), and its toxicological classification is type II (highly toxic) (Fig. 1).

In plants, paraquat interferes with the intracellular electron transfer system, inhibiting reduction of NADP to NADPH during photosynthesis, when the superoxide radical (O_2^-), hydroxyl radical (OH^-) and hydrogen peroxide (H_2O_2) are formed. Studies have suggested that it is these species that are responsible for the tissue damage. They are unstable, and react rapidly with fatty acids, causing lesions in membranes, proteins and DNA. There are no recognized lethal doses of paraquat for animals. However, the average lethal doses (LD50) for oral administration have been

* Corresponding author at: Department of Environmental Engineering, São Paulo State University – UNESP, Avenida Três de Março, no. 511, CEP 18087-180, Sorocaba, SP, Brazil. Tel.: +55 15 3238 3415; fax: +55 15 3228 2842.
E-mail address: leonardo@sorocaba.unesp.br (L.F. Fraceto).

0304-3894/$ – see front matter © 2011 Elsevier B.V. All rights reserved.
doi:10.1016/j.jhazmat.2011.03.057

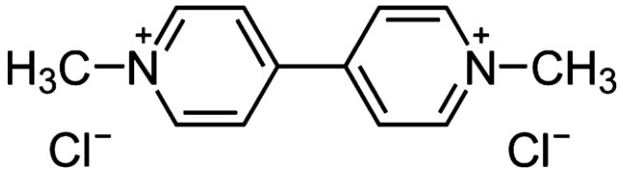

Fig. 1. Chemical structure of paraquat dichloride.

reported to be 35 mg kg^{-1} for cats, 25–50 mg kg^{-1} for dogs and pigs, 50–75 mg kg^{-1} for sheep, and 35–50 mg kg^{-1} for cattle [2].

In recent decades, there has been increasing interest in the use of nanotechnology in agroindustrial applications. Nanoparticles are colloidal size particles with diameters varying from 1 to 1000 nm, where bioactive compounds can be encapsulated, adsorbed or dispersed through the particle matrix. Materials that have been investigated for use as controlled release systems include polymeric substances [5], dendrimers [6], organic microspheres [7], cyclodextrins [8] and natural biodegradable polymers [9,10]. The advance of studies concerning these materials is justified by the advantages they afford, due to their small size. This enables them to reach targets that are normally difficult to access, with increased contact due to their high surface area. Furthermore, nanostructured systems can be optimized in terms of the release rates and dosages of the associated substances [11,12].

The main goals of the use of nanoparticle-based release systems are to maintain the structures and activities of the associated substances, and to release the substances over a longer period. A requirement is that the material composing the particles should produce non-toxic metabolites that can easily degrade. To this end, much attention has focused on colloidal polymeric nanoparticles derived from polysaccharides, lipids and various natural biodegradable polymers. The interaction between cationic and anionic biodegradable polymers, which can produce hydrogels and nanoparticles, provides conditions favorable for the incorporation of chemical substances including agrochemicals and pharmaceuticals. Chitosan and alginate are two polymers that have been used in studies of the release of substances including vaccines, proteins, and drugs to combat tuberculosis, with satisfactory results. Of the various types of complexes with chitosan reported in the literature, the most useful combination for colloidal release systems is chitosan with sodium alginate. The chitosan–alginate (CS–ALG) complex is formed during an ionotrophic gelification process, as a result of interactions between alginate carboxylic groups and chitosan amine groups [13]. Chitosan is commonly obtained by deacetylation of chitin under alkaline conditions. The properties of this polysaccharide include biocompatibility and biodegradability, while its degradation products are non-toxic and non-carcinogenic, so that it can be readily used in many areas of agro-industry [14]. Alginate is an anionic water-soluble linear polysaccharide, composed of 1–4 linear copolymers of β-D-manuronic (M) and α-L-guluronic (G) acids. It is widely used in medicinal applications for controlled release of bioactive compounds, due to its ease of passage through biological barriers, which reduces the toxicity, improves the stability and increases the bioavailability of the associated chemical [13].

Problems arising from the herbicides currently in use relate to their chemical stability, and include issues of solubility, bioavailability, photodegradation and soil sorption. In addition, transfer of these agents to aquatic systems can affect water quality, resulting in adverse impacts to humans, other biota and the wider environment [15–17]. There is therefore a need to develop systems that permit alteration of the physico-chemical properties and release profiles of herbicides, improving soil management and the production of food to meet growing demand, without significant damage to the environment.

The objective of the present work was to prepare alginate/chitosan (AG/CS) nanoparticles, and to characterize their association with paraquat using measurements of size (hydrodynamic diameter), zeta potential (colloidal stability), polymer chemical stability as a function of time (by analysis of solution pH changes), and the percentage loading of the nanoparticles with the herbicide, together with physico-chemical characterization (by transmission electron microscopy, differential scanning calorimetry and Fourier transform infrared spectroscopy). *In vitro* release tests, and sorption tests employing different soils, were used to identify the changes that occurred when the herbicide was associated with the nanoparticles. AG/CS nanoparticles are classically used as carrier systems for pharmaceuticals, however in the present work they were used as a carrier for the herbicide paraquat, since their biodegradability can not only help to reduce environmental impacts, but also assist in the controlled release of the chemical. The ultimate goal was to produce an environmentally safer and more efficient carrier system. A further advantage of AG/CS nanoparticle carrier systems is that they are simple to prepare, which makes them a useful alternative in agricultural applications, as well as elsewhere.

2. Experimental

2.1. Materials

Paraquat dichloride (Pestanal®), chitosan, alginate, AOT (sodium bis(2-ethylhexyl) sulfosuccinate) and 1-hexasulfonic acid (sodium salt) were obtained from Sigma Chemical Company. Methanol was provided by J.T. Baker. Deionized water was supplied from a Milli-Q system (Millipore). All other reagents were of analytical grade. Additional materials used were 0.22 μm polyethersulfone membranes and 30 kDa regenerated cellulose ultrafiltration filters (Millipore), cellulose membranes with molecular exclusion pore size of 12 kDa (Spectrapore), and a centrifuge.

2.2. Methods

2.2.1. Preparation of the alginate/chitosan nanoparticles

The AG/CS nanoparticles were prepared according to the procedure described by Sarmento [18]. Firstly, a sodium alginate solution (0.063%, m/v) was prepared, to which was slowly added 7.5 mL of 18 mM calcium chloride solution, over 60 min with mechanical stirring. Twenty-five milliliter of chitosan solution were then added to the first solution, over 90 min. Preparation of the chitosan solution employed 1 M acetic acid, with agitation for 12 h, due to its low solubility. After preparation, the nanoparticles were stored in an amber flask for subsequent characterization. Paraquat was incorporated in the alginate solution, to a final concentration of 200 μg L^{-1}. Samples of the AG/CS nanoparticles, either with or without paraquat, were lyophilized prior to the DSC and FTIR analyses.

2.2.2. Size and polydispersion measurements

The dynamic light scattering technique was used to determine the average size (as hydrodynamic diameter) and polydispersion of the particles. The analyses were performed with a 1:10 (v/v) dilution of the nanoparticle suspensions, using a Zeta Plus® particle analyzer with detector at a fixed angle of 90° and at a temperature of 25 °C. The size distribution and polydispersion measurements were expressed as the averages of 10 readings [19–21].

2.2.3. Zeta potential measurements

Zeta potential values (mV) were determined using the Zeta Plus® analyzer, after 1:10 (v/v) dilution of the nanoparticle suspensions, and expressed as the average of 10 readings.

2.2.4. AG/CS nanoparticles determined by transmission electron microscopy (TEM)

The suspension of AG/CS nanoparticles was examined in a JEOL 1200EX II microscope (JEOL, Akishima, Japan) operating at 80 kV. In order to perform the TEM observations, the nanoparticles loaded with paraquat were first diluted in water, after which a negative fixation technique was applied [22]. In this technique, the diluted suspension was mixed with 2% uranyl acetate solution; a drop of the mixture was deposited onto a standard copper grid covered by a holey carbon film, and dried at ambient temperature before observation. After evaporation of the liquid, the nanoparticles were fixed on the carbon film of the grid, and could be visualized in the microscope.

2.2.5. Differential scanning calorimetry

Samples (5 mg portions) were placed in pans in a TA Instruments Q100 calorimeter, and heated from 25 to 250 °C, at a scanning rate of 10 °C min^{-1}, under nitrogen flow. An empty pan served as reference, and pure indium was used to calibrate the standard temperature. Measurements were performed for all samples (paraquat, physical mixture of sodium alginate and chitosan polymers, AG/CS nanoparticles, physical mixture of paraquat and AG/CS nanoparticles, and paraquat-loaded AG/CS nanoparticles).

2.2.6. Characterization of microspheres by infrared spectroscopy

The experiments were carried out using an Agilent spectrometer in the range from 400 to 4000 cm^{-1}, with 128 scans per sample and 2 cm^{-1} resolution. Paraquat, the physical mixture of sodium alginate and chitosan polymers, AG/CS nanoparticles, the physical mixture of paraquat and AG/CS nanoparticles, and paraquat-loaded AG/CS nanoparticles were analyzed using KBr pellets.

2.2.7. Chemical stability measurements

Measurement of the pH of the nanoparticle suspensions, as a function of time, was used to examine the chemical stability of the polymers in the formulations [23]. These measurements were continued for a period of 60 days, using a potentiometer calibrated with pH 7.0 and pH 4.0 buffer solutions.

2.2.8. Measurement of the percentage loading of paraquat in the alginate/chitosan nanoparticles

The percentage loading of paraquat in the nanoparticles was determined by the ultrafiltration/centrifugation technique. The samples of nanoparticles containing paraquat were centrifuged in ultrafiltration filters composed of regenerated cellulose with 30 kDa molecular exclusion pore size (Microcon, Millipore), and the filtrate was analyzed using a high performance liquid chromatograph (Varian). The percentage loading was determined as the difference between the concentration of the herbicide in the filtrate and the total concentration (100%) in the nanoparticle suspension [12,23].

The chromatographic analyses were conducted using a mobile phase consisting of 3.5 mL triethanolamine and 1.0 g sodium hexasulfonic acid in 1 L deionized water, at pH 2.5 (adjusted using phosphoric acid) and flow rate of 2.3 mL min^{-1}. Paraquat was separated at 35 °C on a Gemini RP-18 column (150 mm × 4.60 mm, 5 μm, Phenomenex, Torrance, USA), and detected at a wavelength of 257 nm using a UV detector. The injection volume was 20 μL, and all samples were previously filtered through a 0.22 μm membrane. Total paraquat (100%) present in the nanoparticle suspension was determined after diluting the suspension with methanol. This dissolved the polymer, resulting in complete release of the paraquat, which was then quantified from the analytical curve (in a concentration range of 15–55 μM; peak area = 0.1837×10^6[paraquat] − 0.197×10^4, $r = 0.9995$).

Table 1
Characterization of the soil samples obtained from the mid-Rio Negro basin and used in the paraquat soil sorption experiments.

	Iara soil	Carvoeiro soil
Collection depth (cm)	0–10	0–10
Pedological classification	Humic gley	Red–yellow podzol
Characteristics of the region	Locality of Lake Iara, seasonally flooded, dark river water	Forest region, not liable to flooding
Location coordinates	S 01°20.010″ W 062°03.809″	S 01°23.615″ W 061°58.776″
pH	3.4	3.1
Organic matter (%)	24.66 ± 0.30	9.37 ± 0.56
C/N	16.0	18.3
Sand (%)	39.8	54.0
Silt (%)	40.1	34.6
Clay (%)	20.1	11.4

2.2.9. Release of paraquat from the alginate nanoparticles

The release profiles of paraquat, either free or associated with the nanoparticles, were determined using a two-compartment system, with donor and receptor compartments separated by a cellulose membrane with molecular exclusion pore size of 1000 Da, under agitation [24]. The experiment was conducted under dilution "sink" conditions.

Two milliliter aliquots were withdrawn from the receptor compartment at intervals of 15, 30 and 60 min, over a total of 480 min, and quantified by HPLC (using the analytical conditions described for the percentage loading measurements). The receptor compartment was filled with buffer after withdrawal of each aliquot, to maintain a constant volume. The areas of the chromatograms obtained were converted into the percentage of herbicide released, with calibration using a standard solution of free paraquat in water.

2.2.9.1. Mathematical modeling of release profiles. The semi-empirical Korsmeyer–Peppas model [25] was used to analyze the behavior of paraquat release from the alginate nanoparticles. The model is described by:

$$\frac{M_t}{M_\infty} = kt^n \quad (1)$$

where, M_t/M_∞ is the proportion of compound released in time t, k is the kinetic constant, and n is the exponent (which reflects the type of release mechanism). Korsmeyer and Peppas proposed that values of $n \leq 0.43$ are indicative of release mechanisms that follow Fick's Law, while $n > 0.85$ indicates that the mechanisms are governed by relaxation processes, defined as Case II type transport. Intermediate values ($0.43 < n < 0.85$) suggest anomalous behavior, with non-Fickian release kinetics (and a combination of diffusion and relaxation of the polymeric chains).

2.2.9.2. Sorption assays. Soil sorption kinetics experiments were performed by adding 20 mL of 0.01 M $CaCl_2$ solution containing 50 μM of paraquat (either free or associated with the alginate/chitosan nanoparticles) to 0.05 g of soil. The mixture was placed in an Erlenmeyer flask, maintained under agitation (100 rpm) at 25 °C. 1 mL aliquots were periodically removed, and the paraquat content quantified by HPLC (Section 2.2.8). At the same time, 1 mL volumes of 0.01 M $CaCl_2$ were added to the system, to maintain the same volume. The total time period was 3 h, and the tests were performed in triplicate. The aliquots withdrawn were centrifuged for 5 min at 2000 rpm, the supernatant filtered using a 0.22 μm filter, and the paraquat content measured by HPLC. The soil sorption experiments were performed using two different soil types, collected in Amazonia, denoted Iara and Carvoeiro, whose characteristics are described in Table 1.

Table 2
Equations of the sorption kinetics models used in the studies involving paraquat and soils.

Model	Equation	Description
Pseudo-first order	$\log(q_e - q_t) = \log(q_e) - \frac{k_1}{2.303} \times t$	Where k_1 is the pseudo-first order rate constant (μmol g^{-1} min^{-1}), q_e is the amount of paraquat adsorbed at equilibrium (μmol g^{-1}) and q_t is the amount of paraquat adsorbed at time t (μmol g^{-1}).
Pseudo-second order	$\frac{t}{q_t} = \frac{1}{(k_2 \times q_e^2)} + \frac{t_1}{q_e} \times t$	Where k_2 is the pseudo-second order rate constant (μmol g^{-1} min^{-1}), q_e is the amount of paraquat adsorbed at equilibrium (μmol g^{-1}) and q_t is the amount of paraquat adsorbed at time t (μmol g^{-1}).
Intraparticle diffusion	$q_t = k_p \times t^{1/2} + I$	Where k_p (min$^{-\circ.5}$) is the rate constant, I provides an indication of the boundary layer effect and q_t is the amount of paraquat adsorbed at time t (μmol g^{-1}).

Following quantification of the paraquat content of the samples, the soil sorption kinetic curves were constructed, and analyzed using different sorption kinetics models (pseudo-first order, pseudo-second order and intra-particle diffusion) (Table 2). The sorption at equilibrium was calculated as the difference between the herbicide concentration in the initial solution and in the solution after attainment of equilibrium with the soil [26].

2.2.10. Assessment of the influences of organic matter and soil quantity on the sorption of paraquat (either free or associated with the nanoparticles)

The effect of the variables soil organic matter (using the Iara and Carvoeiro soils) and soil mass on paraquat sorption was examined, for both free herbicide and herbicide associated with the alginate/chitosan nanoparticles. Experimental optimization was achieved using a 3^2 factorial design, with the numbers 1, 0 and −1 indicating the levels used. The quantities of organic matter employed for the different levels were 24.66% (100% Iara soil), 17.01% (50% Iara and 50% Carvoeiro) and 9.37% (100% Carvoeiro soil), and three different quantities of soil were used (0.05 g, 0.025 g and 0.01 g). Experiments were performed in duplicate, with aliquots withdrawn after achievement of equilibrium, as described in Section 2.2.10. The data were analyzed using the Statgraphics (v. 5.1) program to obtain the surface responses as well as the influence of each variable on paraquat sorption.

3. Results and discussion

3.1. Characterization and stability of the nanoparticle formulations

Characterization of the alginate/chitosan nanoparticles containing paraquat was achieved using the particle size, zeta potential and pH values of the formulations. The hydrodynamic diameter, zeta potential and polydispersion values were 635 ± 12 nm, −22.8 ± 2.3 mV and 0.518, respectively. The measured particle sizes are in line with values reported in the literature for the preparation method employed [18,27,28]. The zeta potentials are indicative of a system possessing good colloidal stability, since they generally exceed 30 mV [12]. The increase observed in the case of the nanoparticles associated with paraquat could be due to rearrange-

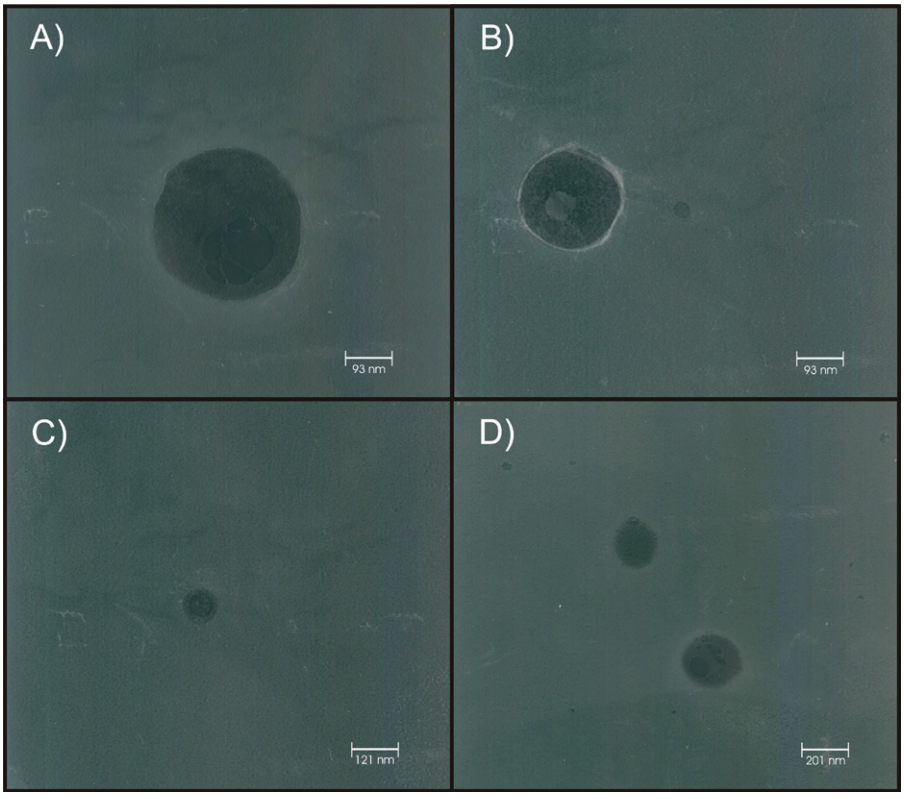

Fig. 2. Transmission electron microscopy images of AG/CS nanoparticles loaded with paraquat. Magnification levels: (A) ×100,000; (B) ×30,000; (C) ×30,000; (D) ×100,000. The bars represent the scale of each image.

ment of the polymeric chains in the presence of the chemical, hence exposing a greater number of ionized groups on the nanoparticle surfaces [18,27]. The polydispersion index values of the AG/CS nanoparticles were high (>0.2), suggesting that the particles did not show good homogeneity, as has been found previously [29].

The morphology of the nanoparticles was analyzed by transmission electron microscopy (Fig. 2), and it was observed that the particles were separate individual spheres in the size range 197–305 nm, with dense, solid structures. Similar features have been observed previously for nanocapsules composed of poly-ε-caprolactone [30]. The sizes of the nanoparticles measured by TEM were smaller than the sizes obtained using the dynamic light scattering (DLS) technique. This apparent discrepancy between the two results can be explained by the dehydration of the AG/CS hydrogel nanoparticles during sample preparation. In addition, DLS measures the apparent size (hydrodynamic radius) of a particle, including hydrodynamic layers that form around hydrophilic particles (such as those composed of AG/CS), leading to an overestimation of particle size. Furthermore, the size distribution of the particles was not homogeneous, as confirmed by the high value of the polydispersivity index (0.518).

The techniques of differential scanning calorimetry and infrared spectroscopy were employed in order to achieve a better characterization of the interaction between paraquat and the AG/CS nanoparticles. The DSC results are shown in Fig. 3, for the rates of heat absorption by paraquat, the physical mixture of sodium alginate and chitosan polymers, AG/CS nanoparticles, the physical mixture of paraquat and AG/CS nanoparticles, and paraquat-loaded AG/CS nanoparticles.

In Fig. 3a, a narrow endothermic peak can be seen at 70 °C, due to fusion of the paraquat. In Fig. 3b and c, broad endothermic peaks can be seen at 62 and 68 °C, for the physical mixture of the alginate and chitosan polymers, and for the AG/CS nanoparticles. These values are in agreement with those reported in the literature [31], and are related to the loss of water associated with the hydrophilic groups of the polymers [18,31]. The thermogram for the alginate/chitosan physical mixture shows a broader endothermic peak at 62 °C, which probably reflects overlap of the two separate endothermic peaks resulting from the individual contributions of the alginate and chitosan polymers.

Fig. 3d shows the results for the physical mixture of AG/CS nanoparticles and paraquat, with an intense broad endothermic peak at 68 °C resulting from the combination of the peaks generated by the herbicide and the alginate and chitosan polymers present in the nanoparticle structure. However, this behavior was not observed in the case of the AG/CS nanoparticles loaded with paraquat, with no evidence of the narrow herbicide peak at around 70 °C, and the presence of only the broad peak corresponding to the AG/CS nanoparticles indicating that the herbicide was well dispersed throughout the nanoparticle matrix. The disappearance of the endothermic peak for paraquat is an indication of the possible interaction of paraquat with the AG and CS polymers composing the nanoparticle structure. This could be due to electrostatic association with the negatively charged carboxylic groups of the alginate polymer, since paraquat is positively charged, or to van der Waals type interactions with the chitosan polymer. It is also possible that spaces between the polymer chains could provide a favorable environment for dispersion of the herbicide within the nanoparticles [18,31].

Infrared spectra were acquired for the samples, in the same way as for the DSC analyses. Fig. 4 shows the absorption spectrum of the paraquat molecule, from which the main bands can be seen at 2990 cm^{-1}, possibly corresponding to an aromatic or alkene =C–H bond (or an alkane C–H bond), at 1633 cm^{-1}, which is associated with the stretching vibration of C=N/C–N, and at 1508 cm^{-1}, due to the weak vibration of $H_3C–N^+$ bonds [32].

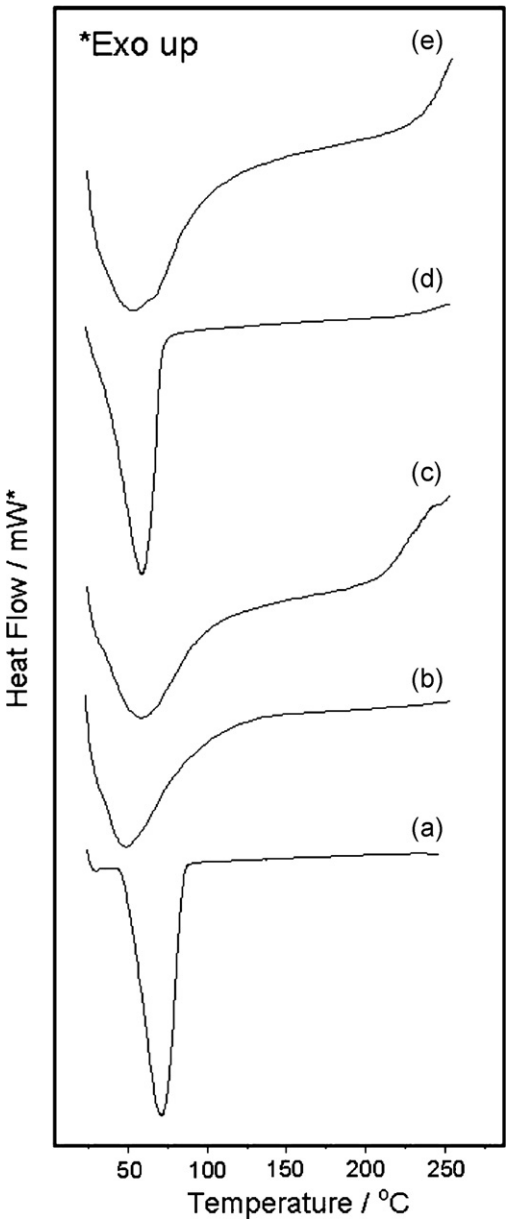

Fig. 3. Differential scanning calorimetry thermograms for pesticide, polymers and nanoparticles. The samples were (a) paraquat; (b) sodium alginate/chitosan physical mixture; (c) AG/CS nanoparticles; (d) AG/CS nanoparticles + paraquat physical mixture; (e) paraquat-loaded AG/CS nanoparticles.

The absorption peaks corresponding to the functional groups present in the alginate and chitosan polymers can be seen in Fig. 4b and c. Peaks near 1612 and 1416 cm^{-1} are associated with the carbonyl groups of alginate (symmetric COO^- stretching vibration, and asymmetric COO^- stretching vibration, respectively). The absorbance peak at 1152 cm^{-1} reflects the amino groups of chitosan. The broad peaks from 1615 to 1609 cm^{-1}, and from 1416 to 1413 cm^{-1}, are observed after complexation of alginate with the chitosan polymer, however no differences were observed between the spectra obtained for the physical mixture of alginate and chitosan polymers and for the AG/CS nanoparticles [32].

Fig. 4d shows the spectrum for the physical mixture of paraquat and AG/CS nanoparticles. The main herbicide absorption bands are present, together with those of the alginate and chitosan polymers. In the case of the herbicide-loaded nanoparticles (Fig. 4e), the characteristic herbicide absorption bands do not appear. This could be indicative of a possible interaction between positively charged

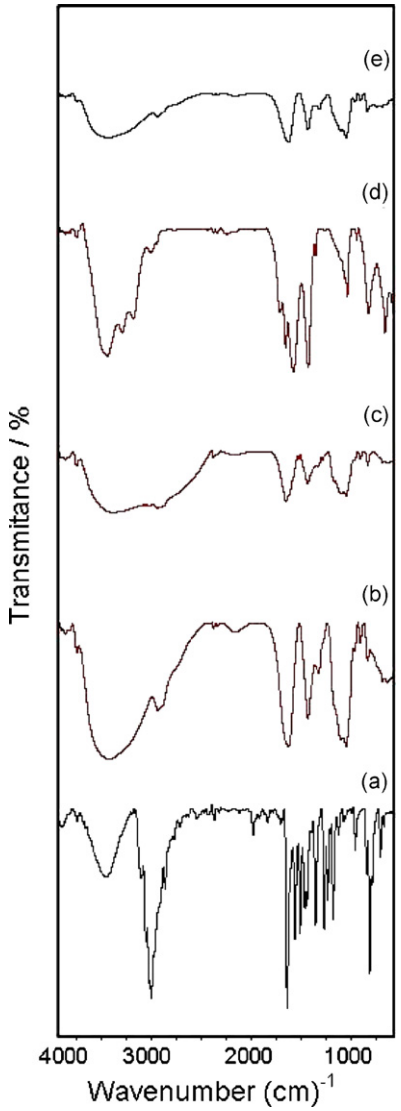

Fig. 4. Fourier transform infrared spectroscopy analysis of the pesticide, polymers and nanoparticles. The samples were (a) paraquat; (b) sodium alginate/chitosan physical mixture; (c) AG/CS nanoparticles; (d) AG/CS nanoparticles + paraquat physical mixture; (e) paraquat-loaded AG/CS nanoparticles.

paraquat groups and the polymer chains (as described previously for the DSC data), with alteration of the herbicide functional group vibrational frequencies, which become superimposed onto those of the nanoparticle polymers [32].

Following initial particle characterization, the chemical stability of the polymers was evaluated by determination of the pH of the formulations as a function of time. After preparation of the AG/CS nanoparticles, the average pH value was 4.85, while an increase to pH 6.11 occurred over the course of 60 days. This significant increase in the pH of the AG/CS formulation could be due to alteration of the equilibrium between the charges present in the alginate and chitosan polymer chains, with time [12].

The percentage loading of the herbicide with the nanoparticles was measured indirectly, using HPLC analyses, considering the difference between the free fraction and the amount (100%) of paraquat used in the preparation. The percentage loading was 74.2%, and was a result of the interaction of the positively charged paraquat molecules with the negatively charged alginate polymers. Alginate is a polyanion, and chitosan a polycation, so that nanoparticles are formed as a result of interlinking of the two polymers. The percentage loading of paraquat in these particles was higher than

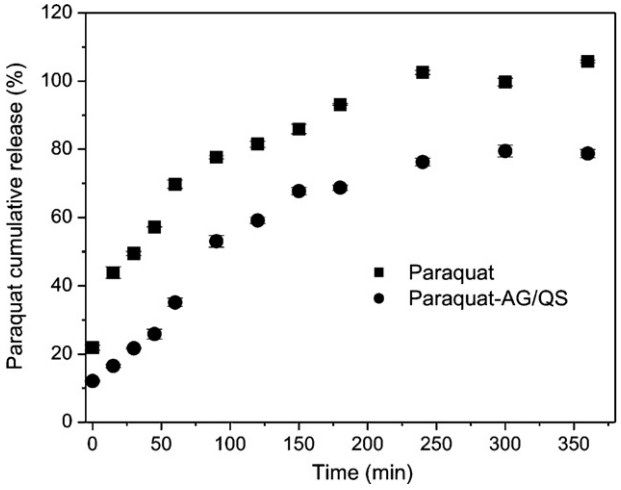

Fig. 5. Release profiles in water of free paraquat and paraquat associated with the alginate/chitosan nanoparticles. The symbols denote experimental data points: (■) paraquat herbicide; (●) paraquat-loaded AG/CS nanoparticles. Experiments were performed at pH 7.4 and 25 °C, and data are expressed as mean ± S.D. (n = 3 experiments).

that reported for the herbicide clomazone (59%) [29]. This difference is due to the presence of charges on the paraquat molecule, in contrast to the highly soluble clomazone, whose chemical structure does not possess any charges.

3.2. Paraquat release assays

Experiments were performed to evaluate the influence of association of paraquat with the nanoparticle polymeric matrices, compared to the herbicide alone (in the absence of nanoparticles). Fig. 5 presents the percentage release curves for paraquat, either free or associated with the AG/CS nanoparticles, as a function of time. The release profile was significantly altered in the presence of the nanoparticles, with near 100% release after 8 h, 2 h longer than the time required for complete release of free herbicide. This alteration of the release profile could be advantageous in use of the herbicide, due to reduction of the amount of the chemical needed to control weeds, as well as reduced environmental risks, lower energy costs (since fewer applications would be required, compared to conventional formulations), and increased safety of the personnel involved in field spraying.

A better understanding of the mechanism of paraquat release from the nanoparticles was obtained by analysis using the Korsmeyer–Peppas model [25]. The release mechanism is dependent on factors including desorption from the surface and diffusion through the pores of the matrix or the polymeric wall, as well as disintegration, dissolution and erosion of the polymeric wall [12,33]. Investigation of the release profile can provide important information concerning the processes governing the release of a chemical [33].

In this model, the relationship between time and the amount of substance released is described by a simple exponential equation, which has been used previously to determine the release of compounds from polymeric systems, especially when the release mechanisms are unknown, or when more than one mechanism is involved [25].

Fig. 6 shows the linearization obtained using the Korsmeyer–Peppas model ($\ln M_t/M_\infty$ as a function of $\ln t$) applied to the release curve of paraquat contained in the AG/CS nanoparticles. The value of the release coefficient (n) was 0.83, which indicates that the release process was governed by mechanisms displaying non-Fickian kinetics, as previously observed for clomazone [29].

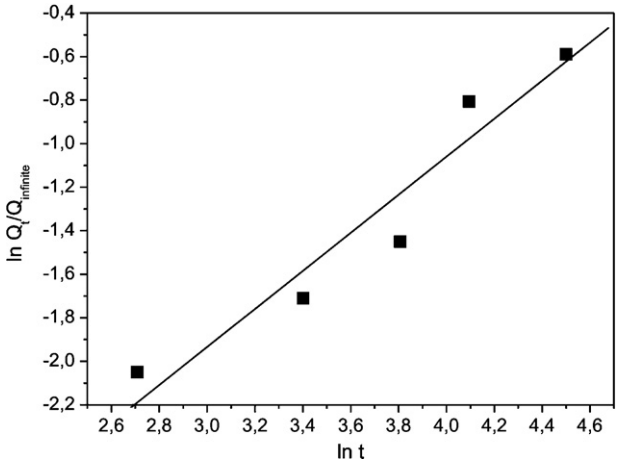

Fig. 6. Linearization of the release curve of paraquat associated with the AG/CS nanoparticles by the Korsmeyer–Peppas mathematical model. The symbol (■) denotes experimental data points, expressed as the mean of three experiments.

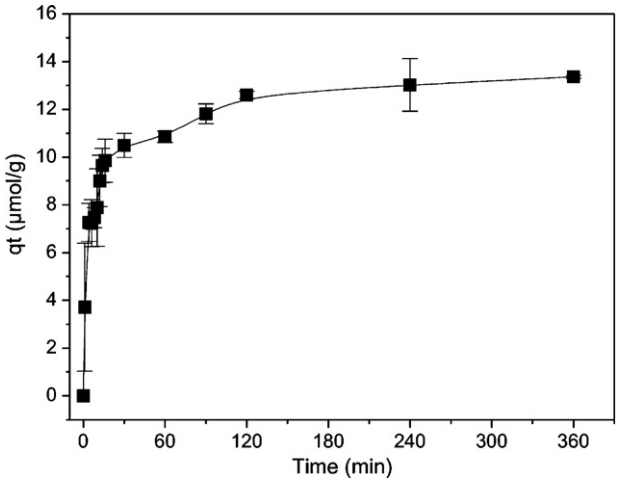

Fig. 7. Sorption isotherm of paraquat herbicide by the Iara soil. q_t is the amount of paraquat sorbed at time t. The symbol (■) denotes experimental data points (25 °C, and the error bars represent the standard deviation of three experiments.

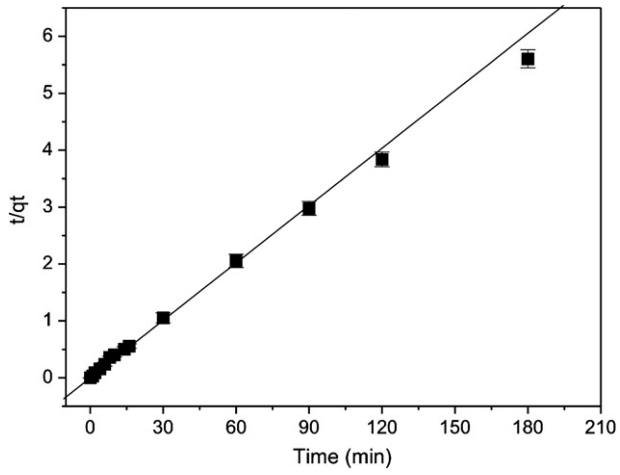

Fig. 8. Pseudo-second order model applied to the sorption isotherm of paraquat with the Iara soil (Fig. 7). q_t is the amount of paraquat sorbed at time t. The symbol (■) denotes experimental data points (25 °C), and the error bars represent the standard deviation of three experiments.

The value of the release constant ($k = 0.012\ \text{min}^{-n}$) was very small, compared to values for other systems described in the literature [29,34,35], and the correlation coefficient was 0.961.

A release system involving paraquat interspersed with aluminosilicate compounds has been described previously [36], where the paraquat molecules were released at a slow rate from the aluminosilicate layers due to ionic interactions between the paraquat and the aluminosilicates. It is likely that the same mechanism may be important in the present case, since release of the paraquat molecules according to the mechanism described above involves the rupture of ionic bonds between the paraquat and the polymeric alginate chains.

3.3. Sorption of paraquat, either free or associated with the alginate/chitosan nanoparticles

Fig. 7 shows that sorption equilibrium was achieved in approximately 120 min, with a decrease in the paraquat concentration from 50 to 2.5 μM after 60 min. Different mathematical models (pseudo-first order, pseudo-second order and intra-particle diffusion) were applied to the kinetic curves in order to obtain information on the adsorption process. The best agreement was obtained using the pseudo-second order model (Fig. 8, Table 3).

The pseudo-second order equation is a model widely applied to sorption kinetics curves, since it describes sorption onto heterogeneous surfaces [37]. As shown in Table 3, this model [38,39] best explained the sorption mechanism, and provided the best linear correlation coefficients (r^2).

The type of kinetics, the kinetic constant (k_2), and the capacity for sorption (q_e) of paraquat by diatomaceous earth and modified clays have previously been found to be similar to the results obtained in the present work using the Iara soil [40,41].

The value obtained for k_2 was directly related to the high initial concentration of paraquat (50 μM), because the greater the initial concentration, the longer the time required to reach equilibrium. Previous work has shown that paraquat has a strong tendency to interact with soil (and other materials) due to its charge, which enables ionic bonding (as well as other bonding mechanisms) since soil organic matter normally possesses predominantly negative surface charge [42–44]. Importantly, where the process is governed by ionic bonding, adsorption of organic compounds and their metabolites involves ionized (or easily ionizable) carboxylic and phenolic hydroxyl groups present in the humic substances [44,45].

Given the reasonable agreement of the experimental results with the pseudo-second order adsorption kinetics model, it can be postulated that the soil presented a variety of different adsorption sites. At these sites, the attachment of paraquat molecules occurs from the aqueous phase, and varies under different environmental conditions. The sorption of paraquat species can reasonably be speculated to occur in two steps: (*i*) Transfer of sorbate present in the aqueous solution to sorbent sites; (*ii*) complexation/ion exchange at the sites. A previous study comparing the influences of pH and salinity on paraquat sorption by charcoal showed that

Table 3
Parameters obtained for the fits of different kinetic models applied to sorption of paraquat by the Iara soil (at 25 °C).

Pseudo-first order			Pseudo-second order			Intra-particle diffusion		
k_1 (μmol g^{-1} min^{-1})	q_e (μmol g^{-1})	r	q_e (μmol g^{-1})	k_2 (μmol g^{-1} min^{-1})	r	k_p	I	r
0.019	14.22	0.877	7.88	0.002	0.999	0.32	8.26	0.931

the sorption process was initially fast, and progressed to a slower second stage until achieving a plateau at equilibrium [42].

Previous studies reported in the literature [43,44] have shown that adsorption of paraquat on a goethite (clay) surface was determined by electrostatic repulsion between paraquat and the positively charged goethite surface, which seemed to be the main factor preventing attachment of the herbicide. However, the presence of humic acid adsorbed onto the goethite surface strongly enhanced paraquat adsorption. In the present study, the Iara soil contained around 25% of organic matter in its composition, enabling it to effectively adsorb paraquat, as shown by the q_e value obtained ($q_e = 7.88\ \mu mol\ g^{-1}$), supporting the existence of ionic bonding between the herbicide and the humic substances present in the soil [37].

3.3.1. Optimization of sorption conditions: factorial design

An experimental optimization was performed for the process of sorption of paraquat (either free or associated with the nanoparticles) by the two different soil types. This considered the influence, on herbicide sorption, of the amount of soil organic matter as well as the quantity of soil. The experimental combinations employed is described in Table 3. The results obtained were analyzed using Statgraphics Plus (v. 5.1). The variable that most influenced sorption of free paraquat was the amount of soil, with a negative effect, while there was a positive influence of the soil organic matter content, as shown in the Pareto graph (Fig. 9A).

The sorption of paraquat increased significantly with increase of the amount of organic matter (the organic matter contents of the Iara and Carvoeiro soils were ~25% and ~10%, respectively) (Fig. 9A), which can be explained by the greater availability of functional groups present in the soil humic substances, and hence of the interaction sites required to increase the paraquat sorption capacity, as explained in section 3.3 [42–44]. From Fig. 9A, it can be seen that increasing the quantity of soil reduced the sorption rate, due to changes in the herbicide/soil ratio. It is notable that there were no observable second order effects arising from the combination of two factors, such as quantity of soil and percentage of organic matter. An empirical linear model (Eq. (2)) was constructed following analysis of the first order paraquat sorption data, using the results of the statistical analysis and the data obtained from the experimental design (Fig. 8). The statistically significant values obtained were fitted by a linear model, using the least squares method ($r = 0.832$):

$$\text{Sorption}\,(\%) = 19.89 + 7.64\,[\text{organic matter}] - 19.89\,[\text{soil mass}], \quad (r = 0.832) \qquad (2)$$

The regression coefficient obtained showed that sorption was significantly and differently influenced by the two factors investigated. From Eq. (2), it can be seen that the soil mass exerted the greatest (negative) influence on sorption of paraquat, while the quantity of organic matter showed a positive effect on soil sorption of paraquat. Hence, the model is capable of predicting the sorption of paraquat in soils, based on the quantity of soil and the percentage of organic matter present.

For comparative purposes, the sorption profile was evaluated for paraquat associated with the AG/CS nanoparticles. The experimental optimization results obtained for the paraquat-loaded AG/CS nanoparticle system are illustrated in the Pareto graph (Fig. 9B). There were no significant changes in percentage sorption for different quantities of soil or organic matter content, indicating that the herbicide remained preferentially associated with the AG/CS nanoparticles, and was not released for sorption by the soil. Physicochemical characterization of the paraquat/AG/CS nanoparticle system by DSC and FTIR showed that the herbicide interacted with the alginate and chitosan chains by electrostatic attraction and van der Waals forces, by means of which it was incorporated into the

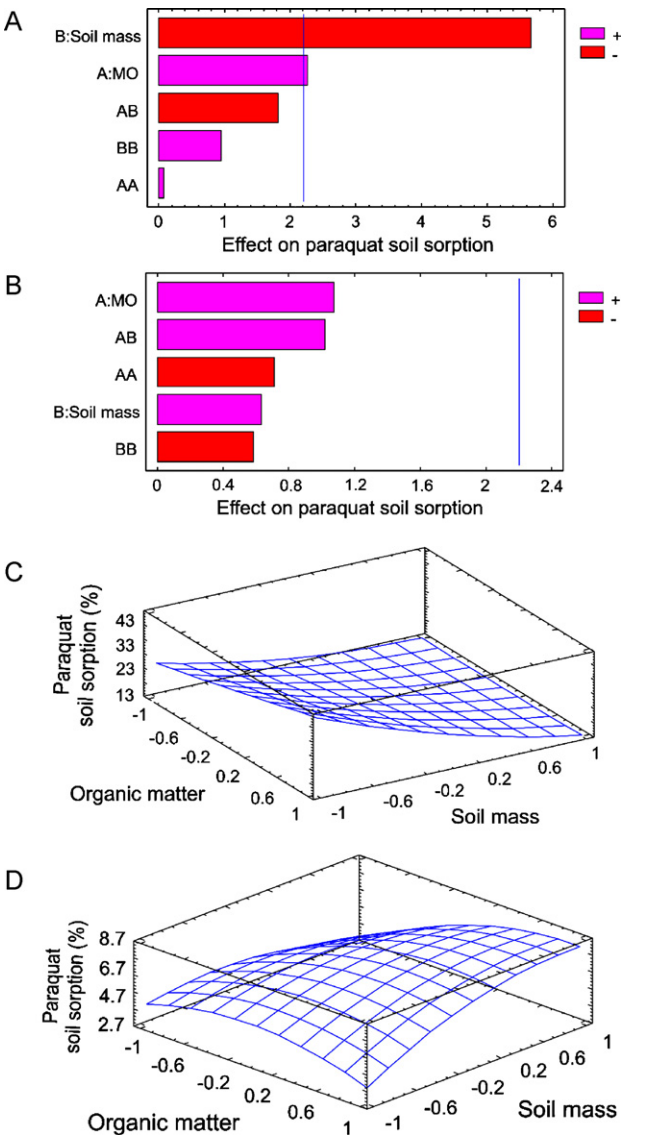

Fig. 9. Optimization of sorption conditions for paraquat herbicide. Influence of soil mass and organic matter percentage on sorption of (A) free paraquat and (B) paraquat associated with the AG/CS nanoparticles. Estimated surface response for sorption of (C) free paraquat and (D) paraquat associated with the AG/CS nanoparticles.

nanoparticle matrix. The strong interaction of paraquat with the nanoparticles inhibited its release for sorption by the soil, so that soil sorption remained low, even after increasing the organic matter content and/or the quantity of the soil.

There are reports in the literature that polymeric materials possessing multiple charges can be used to remove agents such as paraquat from soils, which indicates that the high charge densities of such materials enable desorption of the chemical from the soil, and sorption into the polyelectrolytic polymer matrix [46]. In the present work, the polymers used in the nanoparticle composition (AG and CS) possessed high charge densities, enabling strong interaction with the herbicide (as shown by the DSC and FTIR results) and inhibition of desorption processes that could result in soil sorption, hence explaining the results illustrated in Fig. 9. This feature should greatly improve the availability of the herbicide during use, since secondary processes (such as sorption and degradation) are reduced [41,44].

For comparative purposes, surface response graphs for sorption of paraquat, either free or associated with the AG/CS nanoparticles,

are provided in Fig. 9C and D. From these, it is clear that the herbicide sorption profile is modified according to the method used to apply it to the soil. It is already recognized that the sorption of herbicides can also be influenced by factors including the type of soil, temperature, pH and amount of organic matter present [42,44,47].

4. Conclusions

The results presented here provide valuable information concerning the application of alginate/chitosan nanoparticles as a carrier system for paraquat. The herbicide showed good association with the nanoparticles, which altered its release profile. Sorption tests, using either free or associated paraquat, showed that the soil sorption profile was reduced when paraquat was associated with the nanoparticles, hence improving the herbicidal action. The formulation of paraquat with AG/CS nanoparticles therefore shows promising potential for future use in agricultural applications, offering increased duration of action of the chemical on specific targets, while reducing problems of environmental toxicity.

Acknowledgments

The authors thank FAPESP, CNPq and Fundunesp for financial support.

References

[1] E.D. Armas, R.T.R. Monteiro, P.M. Antunes, M.A.P.F. Santos, P.B. Camargo, Uso de agrotóxicos em cana-de açúcar na bacia do rio Corumbataí e o risco de poluição hídrica, Quim. Nova 30 (2007) 1119–1127.
[2] G.L. Almeida, G.C. Schmitt, A.V. Bairros, T. Emanuelli, S.C. Garcia, Os riscos e danos nas intoxicações por paraquat em animais domésticos, Ciência Rural 37 (2007) 1506–1512.
[3] G. Marchi, E.C.S. Marchi, T.G. Guimarães, Herbicidas: mecanismos de ação e uso, first ed., Embrapa Cerrado, Planaltina, 2008.
[4] USEPA, United State Enviromental Protection Agency, http://www.epa.gov/ (accessed in August 2010).
[5] S. Bogdansky, Natural polymers as drug delivery systems, in: M. Chasin, R. Langer (Eds.), Biodegradable Polymers As Drug Delivery Systems, Marcel Dekker Inc., New York, 1990.
[6] K. Kono, Application of dendrimers to drug delivery systems—from the viewpoint of carrier design based on nanotechnology, Drug Deliv. Syst. 17 (2002) 462–470.
[7] K.S. Soppimath, A.R. Kulkarni, T.M. Aminabhavi, C. Bhaskar, Cellulose acetate microspheres prepared by o/w emulsification and solvent evaporation method, J. microencapsul. 18 (2001) 811–817.
[8] M.B. de Jesus, L.M.A. Pinto, L.F. Fraceto, Y. Takahata, A.C.S. Lino, C. Jaime, E. de Paula, Theoretical and experimental study of a praziquantel and beta-cyclodextrin inclusion complex using molecular mechanic calculations and 1H-Nuclear magnetic resonance, Journal of Pharmaceutical and Biomedical Analysis 41 (2006) 1428–1432.
[9] R. Langer, M. Karel, Controlled release technology: polymers in medicine, food and agriculture, Poly News 7 (1981) 250–258.
[10] M. Fernández-Pérez, E. Villafranca-Sánchez, E. González-Pradas, F. Martinez-López, F. Flores-Céspedes, Controlled release of carbofuran from an alginate-bentonite formulation: water release kinetics and soil mobility, J. Agric. Food. Chem. 48 (2000) 938–943.
[11] K. Letchford, H. Burt, A review of the formation and classification of amphiphilic block copolymer nanoparticulate structures: micelles, nanospheres, nanocapsules and polymersomes, Eur J. Pharm. Sci. 65 (2007) 259–269.
[12] S.R. Schaffazick, S.S. Guterres, L.L. Freitas, A.R. Pohlmann, Physicochemical characterization and stability of the polymeric nanoparticle systems for drug administration, Quim. Nova 5 (2003) 726–737.
[13] S.K. Motwani, S. Chopra, S. Talegaonkar, K. Kohli, F.J. Ahmad, R.K. Khar, Chitosan–sodium alginate nanoparticles as submicroscopic reservoirs for ocular delivery: formulation, optimization and in vitro characterization, Eur, J. Pharmaceut. Biopharmaceut. 68 (2008) 513–525.
[14] N.M. Alves, J.F. Manoa, Chitosan derivatives obtained by chemical modifications for biomedical and environmental applications, Int. J. Biol. Macromol. 43 (2008) 401–414.
[15] J.I. Peréz-Martinéz, M.J. Arias, J.M. Ginés, J.R. Moyano, E. Morillo, P.J. Sánchez-Soto, C. Novák, 2,4-D-cyclodextrin complexes. Preparation and characterization by thermal analysis, J. Therm. Anal. 51 (1998) 965–972.
[16] M. Lezcano, W. Al-Soufi, M. Novo, E. Rodríguez-Nunez, J. Vásquez, Complexation of several benzimidazole-type fungicides with alpha- and beta-cyclodextrins, J. Agric. Food Chem. 50 (2002) 108–112.
[17] M.K. Manolikar, M.R. Sawant, Study of solubility of isoproturon by its complexation with a-cyclodextrin, Chemosphere 51 (2003) 811–816.
[18] B. Sarmento, D. Ferreira, F. Veiga, A. Ribeiro, Characterization of insulin-loaded alginate nanoparticles produced by ionotropic pre-gelation through DSC and FTIR studies, Carbohydr. Polym. 66 (2006) 1–7.
[19] T. Görner, R. Gref, D. Michenot, F. Sommer, M.N. Tran, E. Dellacherie, Lidocaine-loaded biodegradable nanospheres. I. Optimization Of the drug incorporation into the polymer matrix, J. Controlled Release 57 (1999) 259–268.
[20] T. Govender, T. Riley, T. Ehtezazi, M.C. Garnett, S. Stolnik, L. Illum, S.S. Davis, Defining the drug incorporation properties of PLA-PEG nanoparticles, Int. J. Pharm. 199 (2000) 95–110.
[21] S.S. Venkatraman, P. Jie, F. Min, B.Y.C. Freddy, G. Leong-Huat, Micelle-like nanoparticles of PLA–PEG–PLA triblock copolymer as chemotherapeutic carrier, Int. J. Pharm. 298 (2005) 219–232.
[22] F. Leria, R. Marco, F.J. Medina (Eds.), Microscopy, University of Barcelona, 2001, p. 145.
[23] F. Gamisans, F. Lacoulonche, A. Chauvet, M. Espina, M.L. Garcia, M.A. Egea, Flurbiprofen-loaded nanospheres: analysis of the matrix structure by thermal methods, Int. J. Pharm. 179 (1999) 37–48.
[24] A. Paavola, J. Yliruusi, Y. Kajimoto, E. Kalso, T. Wahlström, P. Rosenberg, Controlled release of lidocaine from injectable gels and efficacy in rat sciatic nerve block, Pharm. Res. 12 (1995) 1997–2002.
[25] C. Costa, J.M.S. Lobo, Modeling and comparison of dissolution profiles, Eur. J. Pharm. Sci. 13 (2001) 123–133.
[26] J. Villaverde, C. Maqueda, E. Morillo, Effect of the simultaneous addition of â-cyclodextrin and the herbicide norflurazon on its adsorption and movement in soils, J. Agric. Food Chem. 54 (2006) 4766–4772.
[27] M.D. Chavanpatil, A. Khdair, Y. Patil, H. Handa, G. Mao, J. Panyam, Polymer–surfactant nanoparticles for sustained release of water-soluble drugs, J. Pharm. Sci. 96 (2007) 3379–3389.
[28] R. Grillo, N.F.S. de Melo, D.R. de Araújo, E. de Paula, A.H. Rosa, L.F. Fraceto, Polymeric alginate nanoparticles containing the local anesthetic Bupivacaine, J. Drug Target. 9 (2010) 688–699.
[29] M.S. Silva, D.S. Cocenza, N.F.S. de Melo, R. Grillo, A.H. Rosa, L.F. Fraceto, Nanopartículas de alginato como sistema de liberação para o herbicida Clomazone, Quím. Nova 33 (2010) 1868–1873.
[30] S. Guinebretière, S. Brianon, H. Fessi, V.S. Teodorescu, M.G. Blanchin, nanocapsules of biodegradable polymers: preparation and characterization by direct high resolution electron microscopy, Mater. Sci. Eng. C 21 (2002) 137–142.
[31] K. Mladenovska, O. Cruaud, P. Richomme, E. Belamie, R.S. Raicki, M.C. Venier-Julienne, E. Popovski, J.B. Benoit, K. Goracinova, 5-ASA loaded chitosan-Ca-alginate microparticles: preparation and physicochemical characterization, Int. J. Pharm. 345 (2007) 59–69.
[32] S.T. Hsu, T.C. Pan, Adsorption of paraquat using methacrylic acid-modified Rice husk, Bioresour. Technol. 98 (2007) 3617–3621.
[33] M. Polakovic, T. Gorner, R. Gref, E. Dellacherie, Lidocaine loaded biodegradable nanospheres II. Modelling of drug release, J. Controlled Release 60 (1999) 169–177.
[34] N.F.S. de Melo, R. Grillo, A.H. Rosa, L.F. Fraceto, N.L. Dias Filho, E. de Paula, D.R. de Araújo, Desenvolvimento e caracterização de nanocápsulas de poli (L-lactídeo) contendo benzocaína, Quím. Nova 33 (2010) 65–69.
[35] R. Grillo, N.F.S. de Melo, R. Lima, R. Lourenço, A.H. Rosa, L.F. Fraceto, Characterization of atrazine-loaded biodegradable poly(hydroxybutyrate-co-hydroxyvalerate) microspheres, J. Polym. Environ. 18 (2010) 26–32.
[36] Y. Han, S. Lee, J. Yang, H. Hwang, I. Park, Paraquat release control using intercalated montmorillonite compounds, J. Phys. Chem. Solids 71 (2010) 460–463.
[37] W. Plazinski, W. Rudzinski, A. Plazinska, Theoretical models of sorption kinetics including a surface reaction mechanism: a review, Adv. Colloid Interface Sci. 152 (2009) 2–13.
[38] H. Yuh-Shan, Review of second-order models for adsorption systems, J. Hazard. Mater. 136 (2006) 681–689.
[39] Y.S. Ho, G. McKay, Pseudo-second order model for sorption processes, Process Biochem. 34 (1999) 451–465.
[40] W.T. Tsai, K.J. Hsien, Y.M. Chang, C.C. Lo, Removal of herbicide paraquat from an aqueous solution by adsorption onto spent and treated diatomaceous earth, Bioresour. Technol. 96 (2005) 657–663.
[41] T. Wen-Tien, L. Chi-Wei, Adsorption of herbicide paraquat by clay mineral regenerated from spent bleaching earth, J. Hazard. Mater. 134 (2006) 144–148.
[42] W.T. Tsai, C.W. Lai, K.J. Hsien, The effects of pH and salinity on kinetics of paraquat sorption onto activated clay, Colloids Surf. A: Physicochem. Eng. Aspects 224 (2003) 99–105.
[43] M. Brigante, G. Zanini, M. Avena, Effect of humic acids on the adsorption of paraquat by goethite, J. Hazard. Mater. (2010), doi:10.1016/j.jhazmat.2010.08 028.
[44] K.M Spark, R.S. Swift, Effect of soil composition and dissolved organic matter on pesticide sorption, Sci. Total Environ. 298 (2002) 147–161.
[45] H. Dizer, B. Fischer, I. Sepulveda, E. Loffredo, N. Senesi, F. Santana, P.D. Hansen, Estrogenic effect of leachates and soil extracts from lysimeters spiked with sewage sludge and reference endocrine disrupters, Environ. Toxicol. 17 (2002) 105–112.
[46] F. Sannino, M. Iorio, A. de Martino, M. Pucci, C.D. Brown, R. Capasso, Remediation of waters contaminated with ionic herbicides by sorption on polymerin, Water Res. 42 (2008), 643–562.
[47] A. Iglesias, R. Lopez, D. Gondar, J. Antelo, S. Fiol, F. Arce, Effect of pH and ionic strength on the binding of paraquat and MCPA by soil fulvic and humic acids, Chemosphere 76 (2009) 107–113.